

## DEM SIMULATION OF BALLAST OEDOMETRIC TEST

J. Eliáš\*

**Abstract:** *The granular nature of the railway ballast in connection with fast dynamic loading makes it an ideal application of the Discrete Element Method (DEM). The contribution employs DEM to simulate the ballast behavior in large oedometric test. Ballast grains are represented by convex polyhedral particles with shape randomly generated via Voronoi tessellation. A novel algorithm to compute repulsive contact force based on intersecting volume of polyhedrons is presented. Crushing of grains is included via splitting the particles into smaller polyhedrons when some stress-based criterion is fulfilled.*

**Keywords:** Discrete Element Method, Polyhedrons, Crushing, Voronoi tessellation, Ballast.

### 1. Introduction

Power of modern computers is utilized to help engineers in designing and understanding of their technological solutions more frequently than ever. Dealing with various types of problems led to development of many different methods, among which the Discrete Element Method (DEM) is especially suitable when granular media under highly dynamic loading is studied. DEM treats every grain as an ideally rigid body which interacts with other particles through forces at their common contacts. In most cases, the simplest spherical elemental shapes are used. However, it has been reported that the particle shape has a strong influence on resulting behavior of the system. Therefore, more realistic elemental shapes are being considered. This is often achieved by clumping spheres into some more complex aggregations. Such a method has an advantage in simplicity and computational speed. Another approach lies in direct implementation of some non-spherical elements. There has been also extensive effort to use polyhedral particle shape. A technique developed by Cundall (1988) called *common plane* method is often used. It replaces contact between two polyhedrons by two plane-polyhedron contacts. This method was further improved by fast determination of the *common plane* (Nezami et al., 2006).

The railway ballast is used worldwide to support sleepers and rails on both normal and high speed railways. However, its short and long time behavior is still not fully understood. It is a highly heterogeneous material with strongly nonlinear behavior further complicated by its previous compaction and crushing. Robust models of the ballast are needed for better design of sleepers, under sleeper pads, and ballast itself as well as for determining optimal maintenance schedule of the tracks.

In this contribution, we present simulation of railway ballast experiment - large oedometric test - performed at the University of Nottingham (Lim and McDowell, 2005) using crushable polyhedral particles with random shape. Algorithms presented in the paper were implemented into the open source DEM software YADE (Kozicki and Donzé, 2008). Manipulation with polyhedrons as well as computation of convex hulls and least square fitting by plane is done via open source software CGAL (Kettner, 1999).

### 2. Generation of Randomly Shaped Polyhedral Particles

The particles are created using procedure that contains a random process; however, control of grain size and aspect ratio is kept. Initially, volume of size  $5 \times 5 \times 5$  units is filled by nuclei with minimal mutual distance  $l_{\min}$ . Starting with central nucleus in the center of the volume, other nuclei with random coordinates are accepted if their distance to all previously placed nuclei exceeds  $l_{\min}$ . Voronoi tessellation

---

\* Jan Eliáš: Institute of structural mechanics, Brno University of technology, Faculty of civil engineering, Veveří 331/95; 602 00, Brno; CZ, elias.j@fce.vutbr.cz.

is performed and the Voronoi cell associated with the central nucleus is extracted and used as a basic particle shape. The control of size and aspect ratio is ensured by scaling the Voronoi cell in all three directions according to user defined scaling vector. Finally, the particle is randomly rotated to prevent directional bias. Volume, centroid and inertia of the polyhedral particle is calculated through dividing the polyhedron into tetrahedrons. Contributions of tetrahedrons to each of the wanted quantity are found using analytical formulas.

### 3. Contact between Polyhedrons

In every time step, there is a loop seeking for all possible contacts between polyhedral elements. This is simply done through creation of bounding boxes around every polyhedron and detection of overlapping between the bounding boxes. If bounding box protrudes, one must examine the overlapping of polyhedrons  $\mathcal{P}_A$  and  $\mathcal{P}_B$ . This is solved here through searching for a separation plane.

The polyhedral intersection is assumed to exist until some separation plane is found. Only limited set of candidates for the separation plane must be tested to prove or disprove its existence. The minimal set of candidates contains bounding planes of both of the polyhedrons and planes determined by one edge from  $\mathcal{P}_A$  and another edge from  $\mathcal{P}_B$ . A loop over all these candidates is browsed. Every time, a trial separation plane is constructed so that centroid of the polyhedron  $\mathcal{P}_A$  lies at the positive side of the trial plane. Then, if all vertices from the first polyhedron  $\mathcal{P}_A$  lay at positive halfspace and all vertices from the second polyhedron  $\mathcal{P}_B$  lay in the negative halfspace, the trial plane is approved. If the loop is finished without approving any separation plane, there must be a contact between polyhedrons.

When two grains come into a contact, some repulsive force arises. In DEM simplification, the grains are ideally rigid and the contact is accompanied by overlapping of particles. In case of convex polyhedrons, the intersection is a convex polyhedron as well (Fig. 1). It is denoted  $\mathcal{P}_I$ , its volume is  $V_I$ . It is assumed that in the whole overlapping volume, constant repulsive *volume force* acts. Integrating this *volume force* over the intersecting volume gives us the total *normal force*  $\mathbf{F}_n$  and moment, that should be applied on both particles. Since the *volume force* is constant, the magnitude of the *normal force* is linearly proportional to the intersecting volume

$$|\mathbf{F}_n| = k_n V_I \quad (1)$$

where  $k_n$  [ $\text{N}/\text{m}^3$ ] is a material parameter called volumetric stiffness. To eliminate the moment, the *normal force* acts at the centroid of the intersection. To find the exact polyhedral intersection, dual approach (Muller and Preparata, 1978) is used.

Besides the magnitude of the normal force, its direction must be determined as well. Normal direction is estimated to be perpendicular to a plane  $f$  taken as the least square fit of the shell intersection curve. After polyhedral intersection is found, its faces are divided to those belonging originally to the polyhedron  $\mathcal{P}_A$  and to the polyhedron  $\mathcal{P}_B$ , respectively. Edges on the boundary between these two groups (shell intersection curve) are then interpolated by a plane  $f$  using the least square fitting.

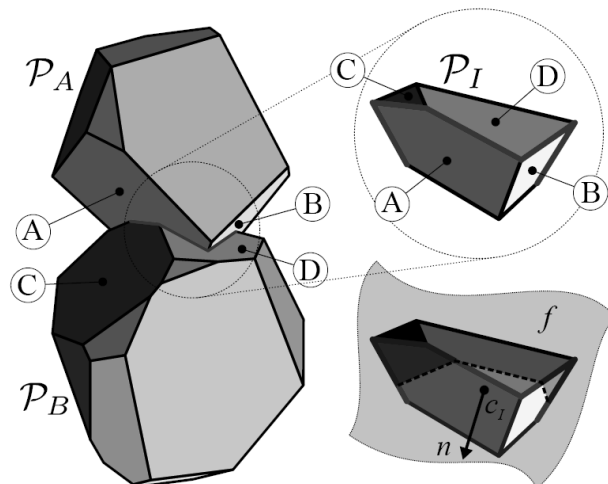


Fig. 1: Two polyhedral particles in contact.

Shear force is calculated by standard incremental algorithm. It consists in correction of the shear force from the last time step for changes in the normal direction and for the rigid-body motion. Then, an additional shear force increment caused by mutual movements and rotations of polyhedrons is added. Standard Coulomb friction is applied. Therefore, the shear force magnitude is limited by magnitude of normal force multiplied by tangent of internal friction angle.

#### 4. Model of Crushing

Crushing of ballast grains is responsible for degradation of ballast and modelling should take it into account. Implementation of the crushing phenomenon is simply done via splitting the polyhedral particles into smaller polyhedrons whenever they fulfill some failure criterion. The criterion is based on comparison of equivalent splitting stress,  $\sigma_e$ , and size dependent strength,  $f_t$ . The average Cauchy stress tensor in the particle can be expressed as

$$\sigma_{ij} = \sum_c l_i^{(c)} F_j^{(c)} \quad (2)$$

where  $c$  runs over all contacts of the particle,  $F^{(c)}$  is a force acting at the  $c$ -th contact at point with spatial coordinates  $l^{(c)}$ ;  $l_i^{(c)}$  and  $F_j^{(c)}$  are  $i$  and  $j$  components of the coordinate vector or force, respectively. The stress tensor is symmetrized by averaging opposite non-diagonal members; then, principle stresses ( $\sigma_I > \sigma_{II} > \sigma_{III}$ ) and their directions are found by eigenvalue analyses. The equivalent splitting stress entering the failure criterion is defined as

$$\sigma_e = -\frac{\sigma_{III}}{2} + \sigma_I \quad (3)$$

The equivalent splitting stress is compared with material strength  $f_t$ , which is (according to Lobo-Guerrero and Ballejo (2005)) dependent on particle size.

Whenever splitting stress exceeds strength of a particle, the polyhedron breaks. Polyhedron is cut through its centroid by two perpendicular planes that are parallel to the second principle stress,  $\sigma_{II}$ , and form angle  $\pi/4$  with the remaining principal stresses. After the breakage, translational and rotational velocities are assigned to the polyhedral pieces according to the current velocities of the original particle.

#### 5. Application to Oedometric Test

The proposed model was validated by simulating a large oedometric test on railway ballast performed and published by Lim and MCDowwel (2005). They tested several different ballasts, from which we chose variant A with ballast of grading 37.5-50 mm. A steel cylinder of diameter 300 mm and depth 150 mm was filled by the ballast and compacted on a vibration table with surcharge force 250 N. Then, it was loaded in compression up to force 1.5 MN (mean stress 21.2 MPa). Total duration of the experiment was about 40 minutes.

The same test was simulated with the polyhedral particles. Initially, randomly shaped polyhedrons were generated at random positions in a cylinder of magnified depth 1 meter with no overlapping. This was done by sequential placing of trial polyhedrons that were rejected whenever any collision with previously placed particles appeared. The polyhedrons then fall freely under 5 times magnified gravitational acceleration and reduced friction angle. Both gravity and friction changes were done to increase compaction of the assembly. After reaching low unbalanced forces, all polyhedrons exceeding depth limit 0.18 m were removed. To increase the compaction, the vibration table was mimicked via loading the sample by alternating acceleration in horizontal directions of magnitude equal to 5 times multiplied gravitation. Each vibration cycle consisted in four intervals of duration 0.02 s with constant acceleration in directions  $+x$ ,  $-x$ ,  $+y$  and  $-y$ , respectively. Three vibration cycles were performed. Then, the simulation continued until low value of unbalanced forces was reached again. At that point, loading by sinusoidal wave started. The loading time was shortened to 1/3 s.

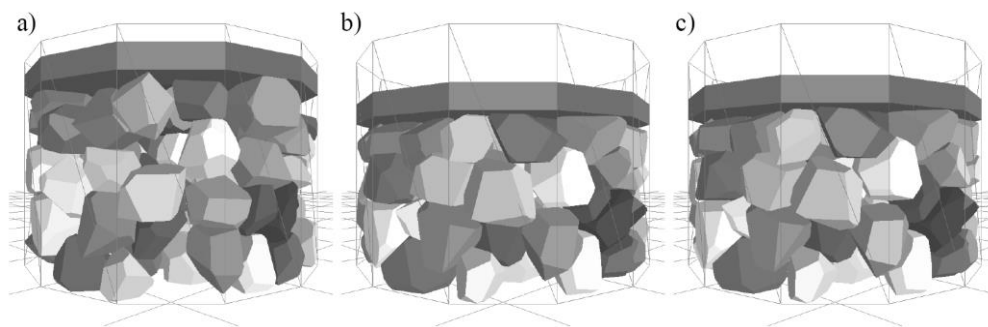


Fig. 2: Snapshots a) at the beginning of loading; b) at the maximum load; c) after releasing all the load.

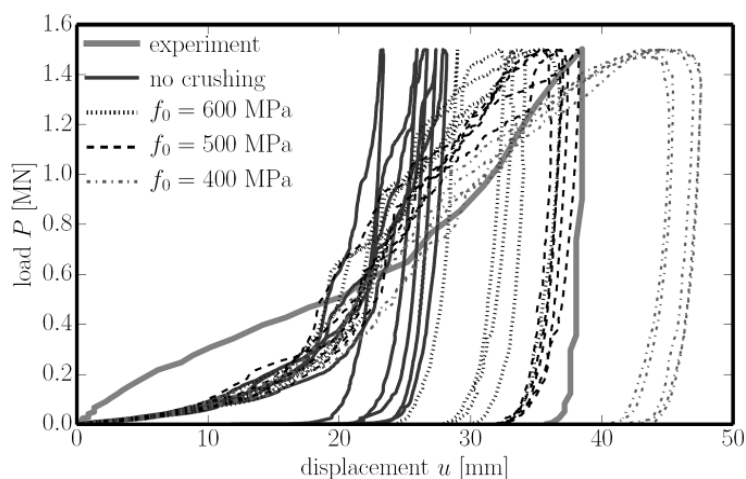


Fig. 3: Load-displacement response of the model with crushable particles.

The shear stiffness and friction angle were estimated; the normal volumetric stiffness of steel was assumed 10 times larger than the ballast normal stiffness, which was approximately identified in Eliáš (2013). Evaluation of the crushing criterion was run every 0.001 s during the simulation. Broken grains with volume lower than 1 cm<sup>3</sup> were removed from the simulation as being less relevant to the overall response but slowing down the simulation substantially. Three variants of strength  $f_0$  were tested: 400 MPa, 500 MPa and 600 MPa. Results are showed in Fig. 3. The value 500 MPa gives the best correspondence with the experimental record. It is interesting that crushing might occur also during unloading, especially for low strength close to the peak load.

### Acknowledgement

The financial support received from Czech Ministry of Education, Youth and Sports under Projects No. CZ.1.07/2.3.00/20.0176 (IRICoN) and LH12062 is gratefully acknowledged.

### References

- Cundall, P. (1988) Formulation of a three-dimensional distinct element model: Part I. A scheme to detect and represent contacts in a system composed of many polyhedral blocks. *Int. J. Rock. Mech. Min.*, 25:107-116.
- Eliáš J. (2013) DEM simulation of railway ballast using polyhedral elemental shapes. In: *Particle-Based Methods III: Fundamentals and Applications*, held in Stuttgart, Germany. pp. 247-256.
- Kettner, L. (1999) Using generic programming for designing a data structure for polyhedral surfaces. *Computational Geometry* 13:65-90.
- Kozicki, J., Donzé, F. (2008) A new open-source software developed for numerical simulations using discrete modeling methods. *Comput. Method. Appl. Mech.* 197:4429-4443.
- Lim, W. L., McDowell, G. R. (2005) Discrete element modelling of railway ballast. *Granular Matter.* 7:19-29.
- Lobo-Guerrero, S., Ballejo, L. E. (2005) Crushing a weak granular material: experimental numerical analyses. *Geotechnique* 55.
- Muller, D. E., Preparata, F. P. (1978) Finding the intersection of two convex polyhedra. *Theor. Comput. Sci.* 7:217-236.
- Nezami, E. G., Hashash, Y. M., Zhao, D., Ghaboussi, J. (2006) Shortest link method for contact detection in Discrete Element Method. *Int. J. Numer. Anal. Met.* 30:783-801.